Organic & Biomolecular Chemistry

ROYAL SOCIETY OF CHEMISTRY

PAPER

View Article Online
View Journal | View Issue

Cite this: *Org. Biomol. Chem.*, 2021, **19**, 6274

Diversity-orientated synthesis of macrocyclic heterocycles using a double S_NAr approach†

Piotr Raubo,* Rodrigo J. Carbajo, William McCoull, Joanna Raubo and Morgan Thomas

Received 30th March 2021,
Accepted 25th June 2021

DOI: 10.1039/d1ob00612f

rsc.li/obc

An efficient macrocyclisation approach based on the double aromatic nucleophilic substitution (SNACK) was developed. This methodology allows a facile incorporation of heterocyclic motifs into macrocyclic rings and rapid synthesis of a significant number of structurally diverse macrocycles. SNACK macrocyclisation enables preparation of stable diastereoisomers of conformationally restricted macrocycles (atropisomers). Practical application of SNACK macrocyclisation in a drug discovery project was exemplified by the identification of high affinity macrocyclic binders of B-cell lymphoma 6 (BCL6).

Introduction

Macrocycles, a class of compounds containing a ring system consisting of 12 or more atoms, are gaining increasing attention within the scientific community. For example, one of the recent issues of Chemical Reviews has been solely devoted to this important chemotype.[1] From a drug design and development perspective, macrocycles occupy a distinctive chemical and property space residing between small molecules and biologics with molecular weights ranging from 400 to 1500 Da.[2] Despite often being outside Lipinski's rule of 5, macrocycles can demonstrate drug-like properties, for example enhanced cell permeability associated with their cyclic conformation and internalisation of polarity can be observed.[3] Indeed, many naturally occurring or synthetic macrocyclic compounds were developed into successful therapeutics, for example: powerful antibiotics, immunosuppressants, antiviral and anticancer agents (Fig. 1).[4]

With the increasing complexity of biological targets macrocyclic molecules provide a promising starting point to modulate challenging targets and interrupt biological pathways. Macrocyclic rings provide a compromise between structural preorganization and sufficient flexibility to fit to a target surface and maximise binding interactions. Thus facilitate modulation of "difficult" targets that contain large, shallow and featureless binding sites such as, for example, protein–protein interactions (PPI).[5] Therefore, macrocycles may be considered as attractive prospective candidates for drug discovery and chemical biology. A macrocyclisation strategy has been often used to lock acyclic ligands capable of selectively modulating the function of biological systems into their bioactive conformation. This can significantly increase potency through maximising polar intermolecular interactions such as hydrogen bonding, minimising entropic cost and improving selectivity against other biological targets.[6,7]

At AstraZeneca, we successfully employed the macrocyclisation approach to lock "acyclic" small molecules into a bioactive conformation, enriching the population of a desired bioactive form and, as a result, significantly improving affinity and selectivity in a number of oncology projects such as, for example, MCL1,[8] BCL6[9] and MTH1.[10]

Despite all the recent advances, macrocycles are still considered a relatively underexploited structural class due to their complex structure and relatively low synthetic tractability. The macrocyclisation step often requires high dilution to favour the macrocyclisation pathway over formation of unwanted intermolecular oligo- and polymerisation side-products.[7,11] Solid-phase synthesis has been also employed as an alternative strategy to achieve pseudo-high dilution conditions for macrocyclisation reactions.[12] In reality, the competition between cyclisation and polymerisation can lead to complex mixtures and reduced overall synthetic efficiency. In the past, as macrocyclic molecules often reside outside Lipinski's rule of 5, they may have been considered as less attractive targets in drug design and candidates for screening library enhancement initiatives. This combined with potentially demanding synthesis may have led to under-representation of macrocyclic structures in screening collections of pharmaceutical companies.[13] The macrocyclic ring can be constructed in a number of ways, using an range of chemical reactions. These strategies were extensively reviewed in literature[6b,14] with a special focus on diversity generating library designs.[2b,13,15] However, there is still a limited number of methods which allow the introduction of diversity within the macrocyclisation step itself. These

Medicinal Chemistry, Research and Early Development, Oncology R&D, AstraZeneca, Cambridge, UK. E-mail: piotr.raubo@astrazeneca.com

†Electronic supplementary information (ESI) available. See DOI: 10.1039/d1ob00612f

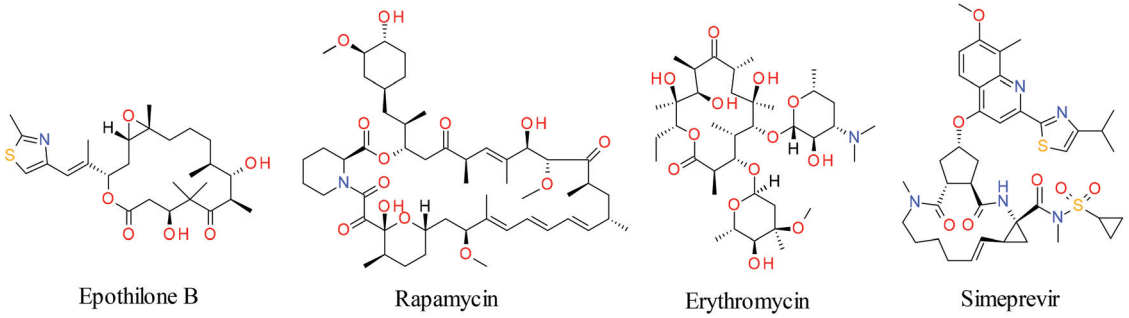

Fig. 1 Selected examples of macrocyclic drugs.

methods are frequently based on multicomponent reactions such as Ugi or Passerini[16] or S_N2 [17] and sometimes on S_NAr processes.[12b,18] Heterocyclic ring systems are often essential elements of many pharmaceuticals and play a significant role in controlling molecular properties such as the electronic distribution, rigidity and three dimensionality as well as modulating physicochemical properties such as lipophilicity, solubility and metabolic stability.[19] Heterocyclic ring systems are also frequently important components of bioactive natural and synthetic macrocycles.[14b,15c,20] Therefore, we were interested in developing a novel, efficient, robust and high yielding method that allowed an expeditious construction of macrocyclic scaffolds to support our medicinal chemistry programs and to expand the AstraZeneca internal screening collection with novel diverse macrocyclic compounds. We aimed for the method to be easily adoptable for automated, parallel synthesis of large arrays of diverse macrocycles. Aromatic nucleophilic substitution (S_NAr) is one of the most widely used reaction in pharmaceutical industry.[21] However, S_NAr appears to be rarely used in the preparation of the synthetic macrocycles.[18] From our standpoint, the double aromatic nucleophilic substitution reaction between pre-assembled, masked di-nucleophiles (**N**) with corresponding heteroaromatic di-electrophiles (**H**) should allow introduction of an element of diversity at the macrocyclisation step, thus facilitating rapid assembly of diverse macrocyclic scaffolds (**M**), ideally in a simple one-pot process (Scheme 1). In this double S_NAr attack (SNACK)[9a] approach the di-nucleophile and di-halo-heterocycle should be easily varied. Importantly, we could also take advantage of the availability of a large set of commercial halogenated heterocyclic building blocks (~90 000, SciFinder), thus comfortably achieving the required structural diversification within the set of constructed macrocyclic rings.

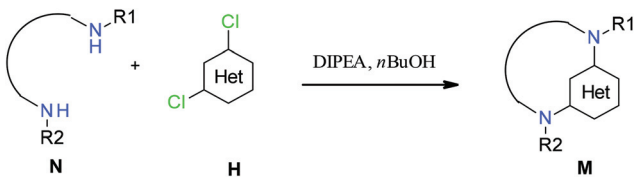

Scheme 1 Double S_NAr attack (SNACK) approach.

Results and discussion

At the outset, to test the possibility of the one-step macrocyclisation, we prepared a model di-nucleophile **N1** (Scheme 2). Boc 3-(*R*)-hydroxypyrrolidine (**1**) first was *O*-alkylated with 1,4-dibromobutane under phase transfer conditions to afford the bromide **2**, which subsequently was used in the second *O*-alkylation with **1** to provide the protected bis-pyrrolidine **3**. Pleasingly, after *N*-Boc deprotection, **N1** underwent dual S_NAr with 2,4,6-trichloropyrimidine (**H1**) to afford the expected 15-membered macrocycle **M1** in 30% yield. The putative side product **4** and other higher oligomers were also detected by LCMS, but were not isolated.

Encouraged by these initial results, **N1** was reacted with a range of heterocyclic di-electrophiles **H2–H10** to obtain a variety of 15-membered macrocycles **M2–M10** in a single step, however, in low isolated yields (Table 1). *Emac* index is a useful descriptor of macrocyclisation efficiency, which takes into account both the chemical yield of the reaction and the concentration at which the macrocyclisation is performed.[22] This index allows comparison of a large number of literature macrocyclisation reactions and enables identification of the most efficient methods. For our unoptimised one step SNACK macrocyclisation reaction *Emac* index was in the low to medium range (*Emac* 4.2–6.5). One of the limitations of the one step process is an inadequate control of regioselectivity of the macrocyclisation, when unsymmetrical reagents are used. A difference in nucleophilicity of both amine centres and dissimilar reactivity of both electrophilic position of the heterocycle is required to avoid formation of isomeric mixtures. For example, the more nucleophilic pyrrolidine **N2** exclusively displaced the more reactive chlorine at the 7-position of 5,7-dichloropyrazolo[1,5-*a*]pyrimidine-3-carbonitrile (**H11**, Table 1). The subsequent S_NAr at the 5-position with the morpholine gave an expected macrocycle **M11** as a single isomer.

N2 was prepared in 3 steps from the 2-hydroxymethyl morpholine **5** as shown in Scheme 3.

To expand the scope of SNACK macrocyclisation, we sought to minimise formation of oligomeric side products and achieve better control of regioselectivity by developing a 3-step procedure. We assumed that using monoprotected di-nucleophiles (*e.g.* ***N*-Boc**) should direct the first aromatic nucleophilic

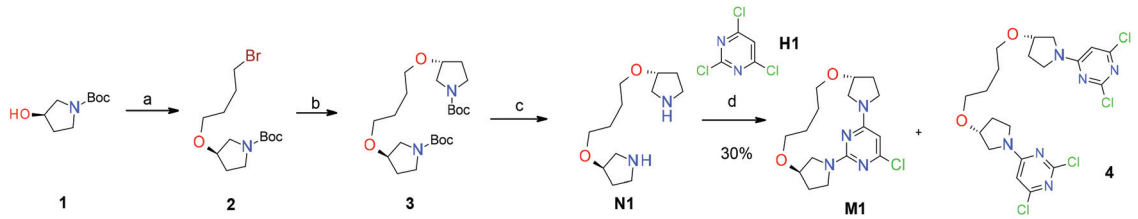

Scheme 2 (a) 1,4-Dibromobutane, *n*-Bu_4HSO_4 cat, PhMe, $NaOH_{aq}$, rt, 86%; (b) **1**, *n*-Bu_4HSO_4 cat, PhMe, $NaOH_{aq}$, rt, 80%; (c) HCl, 1,4-dioxane, EtOH, rt, 99%; (d) **2**, iPr_2EtN, *n*-BuOH, rt-120 °C (<35%).

attack to the more reactive centre of the heterocycle. After subsequent release of the second nucleophile, the second aromatic nucleophilic substitution would take place to form the expected macrocycle **M** (Scheme 4).

To test this concept, we prepared the orthogonally protected di-pyrrolidine **9** (Scheme 5). Selective mono-deprotection of the *N*-Cbz group in **9** afforded the mono-*N*-Boc-protected bis-pyrrolidine **N3** in good overall yield. In the next step, **N3** was set to react with 2,4,5-trichloro-pyrimidine (**H8**) in *iso*-propanol at 80 °C. After completion, the reaction mixture was acidified with excess of methanesulfonic acid and the resulting mixture was heated until full *N*-Boc deprotection. After basification with Hunig's base and dilution, the reaction mixture was subsequently heated within the microwave reactor to provide the expected macrocycle **M8**, pleasingly, in good isolated yield (73%, for a 3 step sequence). Furthermore, we used **N3** in several more macrocyclisations with other heterocyclic coupling partners (**H9–H11**) to obtain corresponding 15-membered macrocyclic compounds **M9–M13**. This procedure significantly improved isolated yields over the one-step experiments (*e.g.* 73% *vs.* 31% for **M8** and 55% *vs.* 12% for **M10**, Table 2).

To demonstrate the scope of our SNACK approach, a set of diverse masked di-nucleophiles was prepared using well established chemistry. The aniline base di-nucleophiles **N4** and **N5** were synthesised as drawn in Scheme 6. (*R*)-*N*-Boc-3-hydroxyproline (**1**) was allylated with (*E*)-1,4-dibromobut-2-ene to form the allyl bromide **10**, which in turn, was used to *O*-allylate the corresponding 3-nitro- and 2-nitrophenol to afford *meta*- and *ortho*-substituted nitrobenzenes **11** and **12** in excellent isolated yields (98% and 95%, respectively). Finally, the nitro group in **11** and **12** was reduced to provide the anilines **N4** and **N5**.

The aniline **N4** was set to react in our 3-step SNACK macrocyclisation with a range of di-chloro-heterocycles (**H1**, **H8**, **H9**, **H11–H22**, Table 2). The reaction between **N4** and 2,4,5-trichloropyrimidine (**H8**) provided the expected macrocycle **M14** in excellent yield. Similarly, macrocyclisation of **N4** with **H1** and **H11** proceeded smoothly affording corresponding macrocyclic structures **M15** and **M16** in 78% and 86% yield, respectively. In the case of **M16** a mixture of 3 possible isomers was obtained in a ratio ~5 : 2 : 2 with **M16** being the major isomer. There are several practical aspects that must be considered to achieve good overall yields for this SNACK macrocyclisation. Firstly, purity of the di-halo heterocycles is important, because of the impact on stoichiometry of the first nucleophilic addition. Excess of one of the reagents, or incomplete first nucleophilic substitution, generally leads to formation of side products at the second nucleophilic addition step. Secondly, variation in relative reactivity of both the nucleophile and electrophile required careful monitoring to ensure complete conversions for the first S_NAr. For more electron rich heterocycles higher reaction temperature or/and longer reaction time was required to achieve acceptable conversion of both nucleophilic substitutions. This sometimes led to more complex reaction profiles and, in consequence, lower overall yields. For example, for **M17**, the first reaction of our SNACK sequence progressed cleanly, albeit very slowly (90 h at 100 °C). However, after the deprotection, the second nucleophilic substitution was much slower and by-products were observed, providing **M17** in only 17% isolated yield. In the attempt to make the macrocycle **M18**, the aniline **N4** did not react with **H9** at the first step of the sequence at all. However, **H9** reacted with the more nucleophilic pyrrolidine **N3** to give **M9**, albeit in 32% yield. Furthermore, SNACK macrocyclisation between **N4** and **H14** and **H15** provided the corresponding 17- and 16-membered macrocycles **M19** and **M20** in moderate yields. For very electron deficient and reactive heterocycles such as the triazine **H16**, *iso*-propanol was replaced with dichloromethane to avoid side reactions with protic solvent. Trifluoroacetic acid was then used for the *N*-Boc deprotection and **M21** was obtained in 38% yield. In our standard macrocyclisation conditions, the 2,5-dichloropyrimidine **H17** reacted with the aniline **N4** to allow incorporation of the pyrimidine ring into the macrocycle ring in **M22**. Furthermore, the reaction between **N4** and the 4-fluoro-substituted **H18** or the 4-chloro-substituted **H19** provided corresponding macrocycles **M23** and **M24** in modest isolated yields (45–52%). However, the attempt to make **M25** from the corresponding 4,6-dichloro-5-(difluoromethyl)pyrimidine was unsuccessful. The first nucleophilic substitution worked very well, as did the amine deprotection. Disappointingly, the macrocyclisation step failed to provide the required difluoromethyl analogue **M25** due to instability of the macrocyclic product. An isomeric *ortho*-substituted aniline **N5** (prepared as shown in Scheme 6) worked well in our SNACK macrocyclisation. The reaction of **N5** with heterocyclic partners such as **H8**, **H14**, **H19** delivered the corresponding macrocycles **M26**, **M27** and **M28** in high overall yields (79%, 76%, 69%, respectively). In the case of **M28**, we observed formation of 2 isomeric products at the final macrocyclisation step. The isomer ratio was

Table 1 One step macrocyclisation

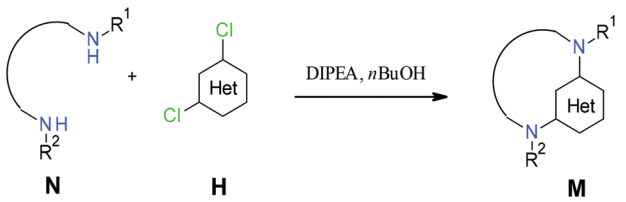

Di-nucleophile	Heterocycle	Di-halo-heterocycle	Macrocycle	Structure	Yield (%)	Ring size	E_{mac}
N1	**H1**	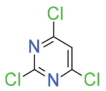	**M1**	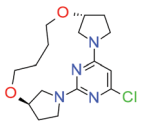	30	15	5.4
N1	**H2**	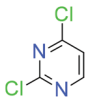	**M2**	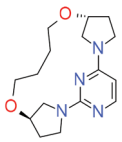	35	15	6.2
N1	**H3**	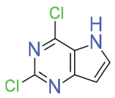	**M3**	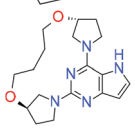	26	15	5.3
N1	**H4**	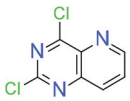	**M4**	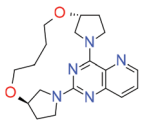	21	15	5.0
N1	**H5**	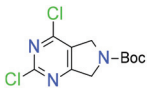	**M5**	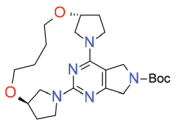	22	15	5.0
N1	**H6**	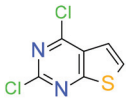	**M6**	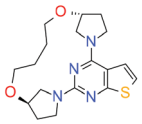	16	15	4.6
N1	**H7**	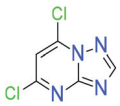	**M7**	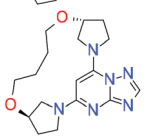	16	15	4.6
N1	**H8**	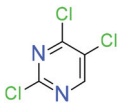	**M8**	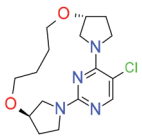	31	15	6.1
N1	**H9**	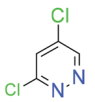	**M9**	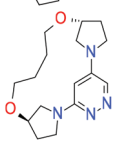	27	15	5.9
N1	**H10**	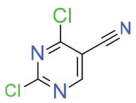	**M10**	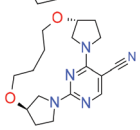	12	15	4.2
N2	**H11**	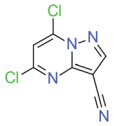	**M11**	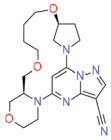	26	15	6.0

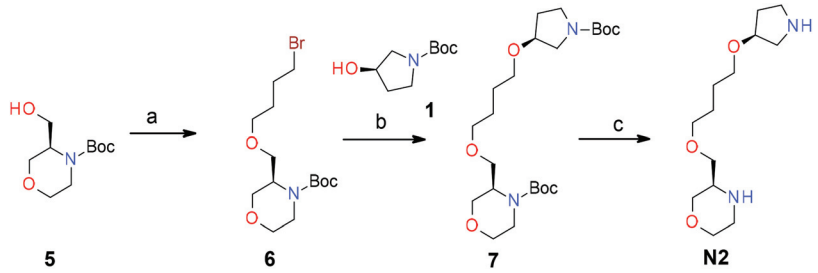

Scheme 3 (a) 1,4-Dibromobutane, n-Bu_4HSO_4 cat, PhMe, $NaOH_{aq}$, rt, 94%; (b) **1**, n-Bu_4HSO_4 cat, PhMe, $NaOH_{aq}$, rt, 73%; (c) HCl, 1,4-dioxane, EtOH, rt, quant.

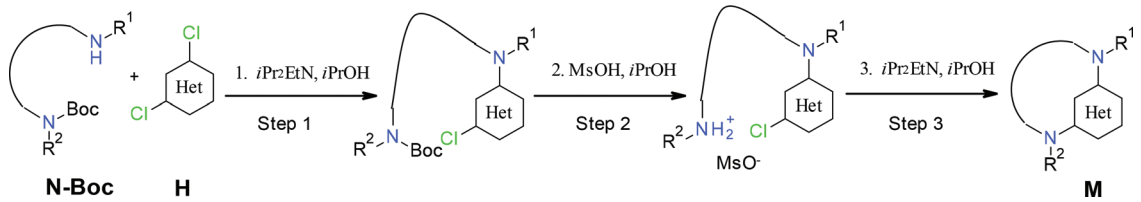

Scheme 4 Three-step SNACK macrocyclisation.

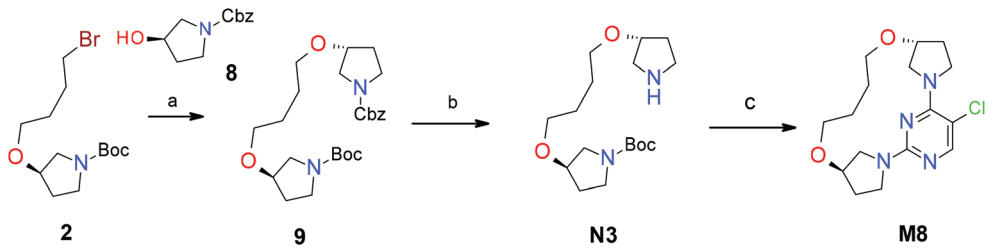

Scheme 5 (a) 1,4-Dibromobutane, n-Bu_4HSO_4 cat, PhMe, $NaOH_{aq}$, rt, 76%; (b) H_2, Pd/C, THF–H_2O, rt, 99%; (c) **H8**, iPrOH, iPr_2EtN, 80 °C; then MsOH, iPrOH, 80 °C; then iPr_2EtN, iPrOH, 120 °C, 73%.

improving with longer reaction time and, after completion, this sequence gave a 17 : 1 mixture of 2 isomeric macrocycles **M28** in 69% overall isolated yield. To explore the scope of SNACK macrocyclisation further, *O*,*O*-butylene linked pyrrolidines **N6**, **N7** and **N8** were prepared in a 3-step sequence from the commercial chiral building blocks (**13**, **14** and **15**, respectively) in excellent overall yields (Scheme 7).

Similarly, the analogous piperidine **N9** was synthesised. The macrocyclisations performed using **N6** and the heterocycles **H8** and **H11** were comparably efficient to the reactions of alkene **N4** giving the expected macrocycles **M29** and **M30** in high yields (64% and 81%, respectively, Table 2). SNACK macrocyclisation between **N7** and **H18** proved to be more sluggish leading to lower efficiency (E_{mac} 5.1) and, as a result, low chemical yield (**M31**, 25%). Similarly, the reaction between a more sterically hindered prolinol **N8** and **H8** was significantly less efficient (**M32**, 30%, E_{mac} 5.5). While the piperidine **N9** underwent smooth macrocyclisation with **H11** to give **M33** in 72% yield, the second nucleophilic substitution at the 6-position of 5-aza-quinazoline **H14** was very slow even at 150 °C and thus low yielding (**M34**, 9%). This may be due to higher ring strain and/or lower nucleophilicity of the piperidine nitrogen in comparison to the corresponding pyrrolidine. Interestingly, the prolinol **N10** bearing the conformationally more defined unsaturated linker was significantly more efficient in SNACK macrocyclisation (E_{mac} 6.8) when compared to the saturated chain linked **N8**. **N10** was quickly assembled as depicted in Scheme 8 and allowed to react with the di-electrophile **H11** to provide a 16-membered macrocycle **M35** in excellent yield (81%).

In order to evaluate the scope of macrocyclisation, more precursors were quickly prepared. Both the amide linked aniline **N11** and **N12** were easily made from the commercially available carboxylic acid **25** and corresponding amines **26** and **28** (Scheme 9).

Furthermore, the one-pot double aromatic nucleophilic substitutions with 2,4,5-trichloropyrimidine allowed swift assembly of the pyrimidine linked primary amines **N13** and **N14** as shown in Scheme 10.

Two isomeric morpholines **N15** and **N16** were prepared from **6** using standard procedures (Scheme 11).

The spirocyclic masked di-nucleophile **N11** smoothly reacted with the heterocyclic reagents **H8** and **H11** forming

Table 2 One-pot three-step macrocyclisation

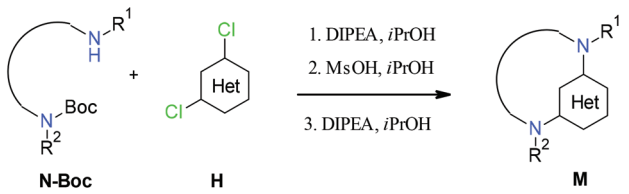

Di-nucleophile	Heterocycle	Di-halo-heterocycle	Macrocycle	Structure	Yield (%)	Ring size	E_{mac}
N3	**H8**	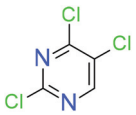	**M8**	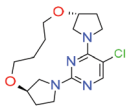	73	15	6.5
N3	**H9**	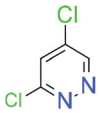	**M9**	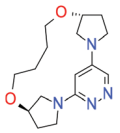	32	15	5.5
N3	**H10**	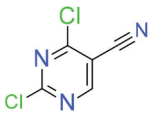	**M10**	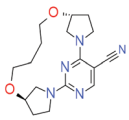	55	15	6.1
N3	**H11**	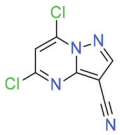	**M12**	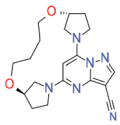	44	15	5.9
N3	**H12**	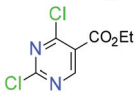	**M13**	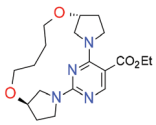	42	15	6.1
N4	**H8**	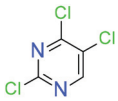	**M14**	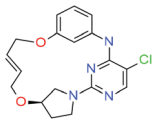	86	16	6.8
N4	**H11**	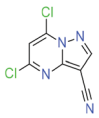	**M15**	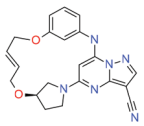	78	16	6.7
N4	**H1**	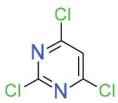	**M16**	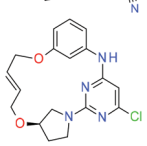	86[a]	16	6.8
N4	**H13**	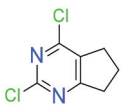	**M17**	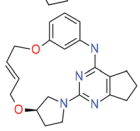	17	16	4.7
N4	**H9**	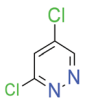	**M18**	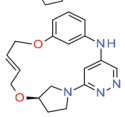	0	NA	NA
N4	**H14**	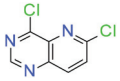	**M19**	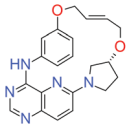	50	17	6.0

Table 2 *(Contd.)*

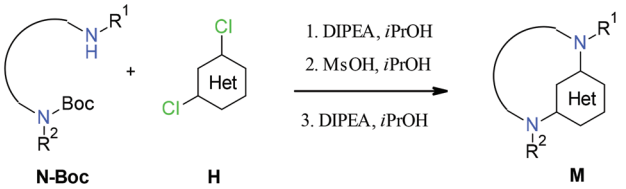

Di-nucleophile	Heterocycle	Di-halo-heterocycle	Macrocycle	Structure	Yield (%)	Ring size	E_{mac}
N4	**H15**	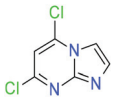	**M20**	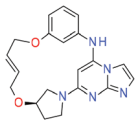	55	16	6.2
N4	**H16**		**M21**	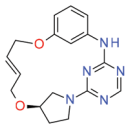	38[b]	16	6.0
N4	**H17**		**M22**	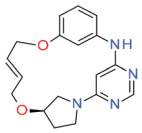	42	16	5.9
N4	**H18**	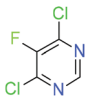	**M23**	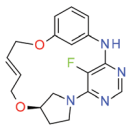	52	16	6.2
N4	**H19**		**M24**	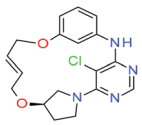	45	16	6.0
N4	**H20**	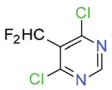	**M25**	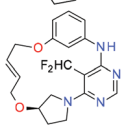	0	NA	NA
N5	**H8**	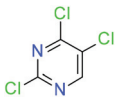	**M26**	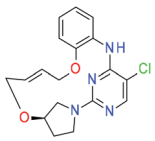	79	15	6.7
N5	**H14**	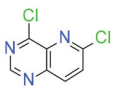	**M27**	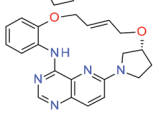	77	16	6.6
N5	**H19**		**M28**	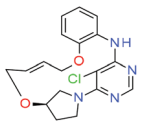	69[c]	15	6.5
N6	**H8**	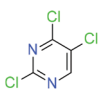	**M29**	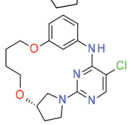	64	16	6.4
N6	**H11**	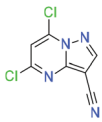	**M30**	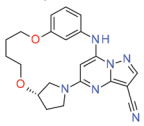	81	16	6.8

Table 2 *(Contd.)*

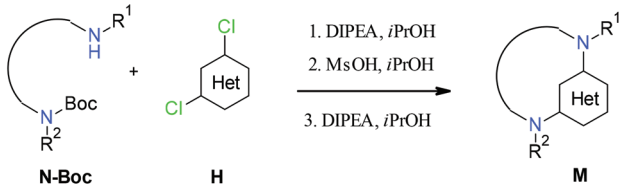

Di-nucleophile	Heterocycle	Di-halo-heterocycle	Macrocycle	Structure	Yield (%)	Ring size	E_{mac}
N7	**H18**		**M31**	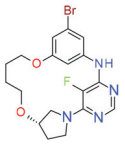	25	16	5.1
N8	**H8**	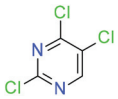	**M32**	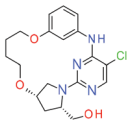	30	16	5.5
N9	**H11**	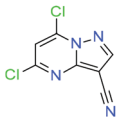	**M33**	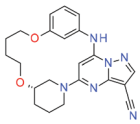	72	16	6.5
N9	**H14**	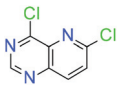	**M34**	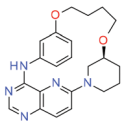	9	17	3.9
N10	**H11**	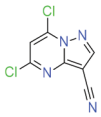	**M35**	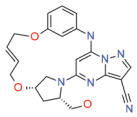	81	16	6.8
N11	**H8**	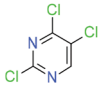	**M36**	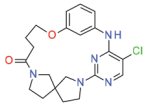	68	17	6.5
N11	**H11**	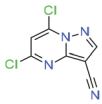	**M37**	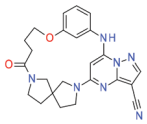	73	17	6.6
N12	**H8**	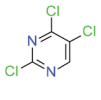	**M38**	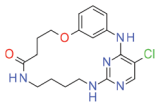	53	18	6.2
N12	**H21**	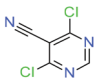	**M39**	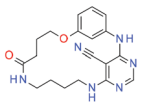	32	18	5.5
N13	**H11**	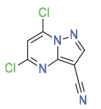	**M40**	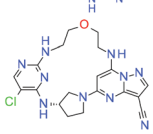	76	17	6.6
N14	**H14**	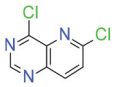	**M41**	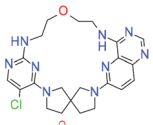	44	19	5.9
N14	**H21**	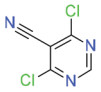	**M42**	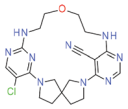	31	18	5.4

Table 2 *(Contd.)*

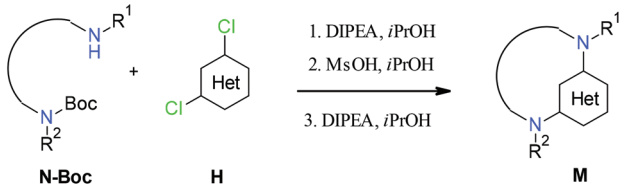

Di-nucleophile	Heterocycle	Di-halo-heterocycle	Macrocycle	Structure	Yield (%)	Ring size	E_{mac}
N14	**H22**	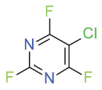	**M43**	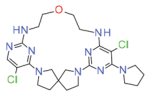	20[d]	18	NA
N15	**H8**	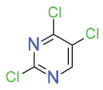	**M44**	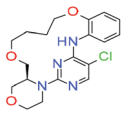	51	15	6.3

General procedure: Di-halo-heterocycle (**H**, 0.18 mmol) was added to a stirred solution of mono-*N*-Boc protected diamine (***N*-Boc**, 0.18 mmol) and DIPEA (0.05 mL, 0.29 mmol) in iPrOH (2 mL). The reaction mixture was stirred at 20–80 °C[a] until completion. Methanesulfonic acid (0.1 mL, 1.54 mmol) was added and mixture was stirred at 60–80 °C[a] until completion. The mixture was diluted with iPrOH (15 mL) and further DIPEA (0.6 mL, 3.44 mmol) was added. The mixture was stirred at 20–150 °C[a] and cooled to rt. The mixture was concentrated *in vacuo* and purified by reverse phase HPLC to afford **M**. (a) *Microwave reactor was used to heat the reaction vessel when necessary.* [a] Total yield for 3 possible regioisomers. [b] For this reactive heterocycle the sequence was carried out stepwise: the first step was performed in dichloromethane, then the Boc group removed with trifluoroacetic acid in dichloromethane and the macrocyclisation step was performed in *iso*-propanol at room temperature. [c] 17 : 1 mixture of 2 diastereoisomers. [d] Overall isolated yield for 4-step one-pot procedure.

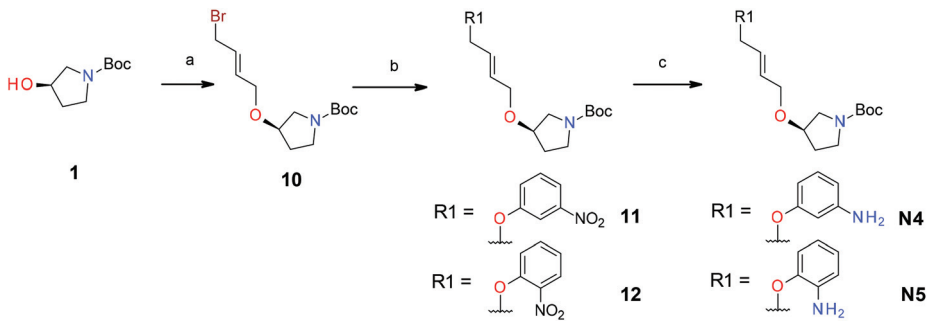

Scheme 6 (a) (*E*)-1,4-Dibromobut-2-ene, *n*-Bu_4HSO_4 cat, PhMe, $NaOH_{aq}$, rt, 78%; (b) 3-nitrophenol, K_2CO_3, DMF, 80 °C, 98% or 2-nitrophenol, K_2CO_3, DMF, 80 °C, 95%; (c) Fe, NH_4Cl, 2-MeTHF, H_2O, 60 °C, for **N4** quant., for **N5** 91%.

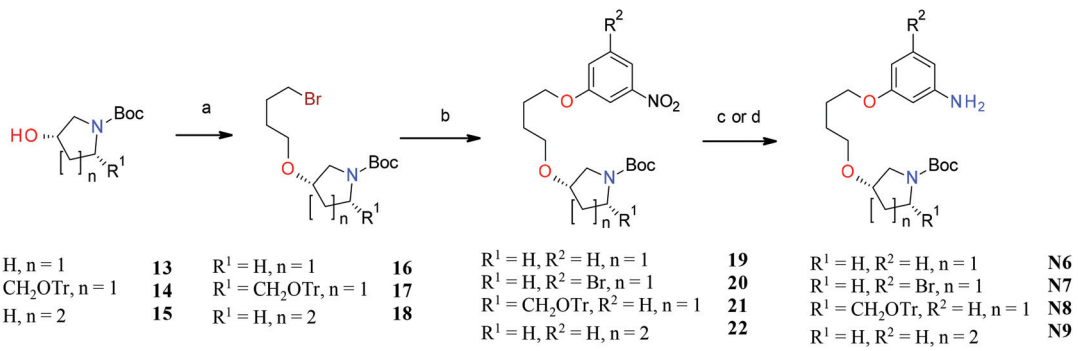

Scheme 7 (a) 1,4-Dibromobutane, *n*-Bu_4HSO_4 cat, PhMe, $NaOH_{aq}$, rt; for **16** 88%; for **17** 93%; for **18** 82%; (b) 3-nitrophenol or 3-bromo-5-nitrophenol, Cs_2CO_3, DMF, 80 °C; for **19** 82%; for **20** 81%;[9b] for **21** quant.; for **22** 92%; (c) $HCOONH_4$, Pd/C, EtOH, 80 °C; for **N6** quant.; for **N8** 95%; for **N9** 96%; (d) Fe, NH_4Cl, 2-MeTHF, H_2O, 75 °C, for **N7** 94%.[9b]

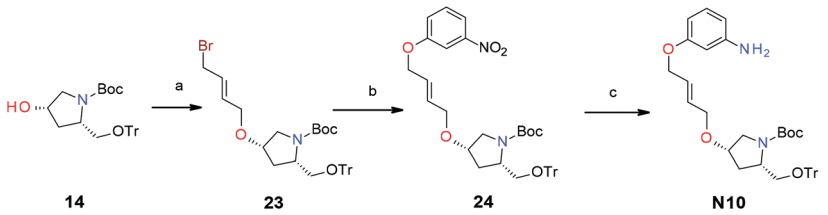

Scheme 8 (a) (*E*)-1,4-Dibromobut-2-ene, *n*-Bu_4HSO_4 $_{cat}$, PhMe, $NaOH_{aq}$, rt, 65%;[9b] (b) 3-nitrophenol, K_2CO_3, DMF, 80 °C, 95%; (c) Fe, NH_4Cl, 2-MeTHF, H_2O, 60 °C, 91%.

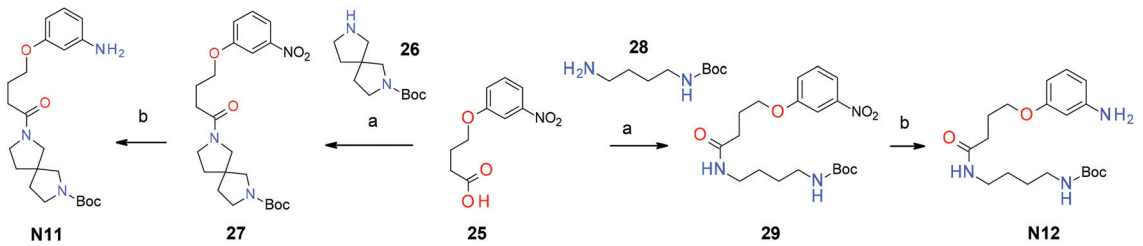

Scheme 9 (a) HATU, iPr_2EtN, DMF, rt, 78% for **27**, 81% for **29**; (b) $HCOONH_4$, Pd/C, EtOH, 80 °C, quant. both for **N11** and **N12**.

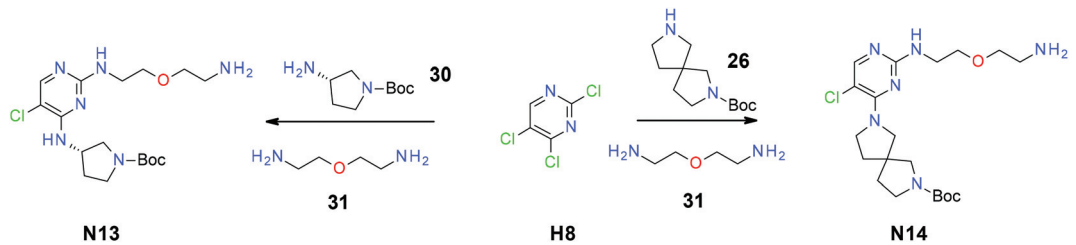

Scheme 10 (a) **30**, iPr_2EtN, i-PrOH, 80 °C; then **31** 120 °C, 75%; (b) **26**, iPr_2EtN, i-PrOH, 80 °C; then **31** 120 °C, 61%.

corresponding spirocyclic macrocycles **M36** and **M37** in good overall yields (68% and 73%, respectively). The macrocyclisation step between the primary amine in **N12** and the heterocyclic partners **H8** and **H21** was less efficient. In this case, expected macrocycles **M38** and **M39** were isolated in modest to low yields (53% and 32%, respectively). Compounds containing two heterocyclic units incorporated into the larger macrocyclic ring, such as **M40**, **M41** and **M42**, where rapidly assembled from the corresponding amines (**N13** and **N14**) and relevant heterocyclic partners **H11**, **H14** and **H21** in two simple separate steps involving four S_NAr reactions. As previously, macrocyclisation with the pyrazolopyrimidine **H11** proved to be efficient for the 17-membered **M40** (yield 76%). However, in the case of the 5-azaquinazoline **H14**, formation of the 19-membered macrocyclic ring in **M41** was less effective (44% yield). As previously found, the SNACK macrocyclisation with 5-cyano-1,6-dichloropyrimidine (**H21**) was less successful affording the 18-membered macrocycle **M42** in 31% yield only.

The SNACK procedure employing heterocyclic reagents bearing three leaving groups can easily expand structural diversity of prepared macrocycles. In the case of 5-chloro-2,4,6-trifluoropyrimidine (**H22**) and **N14** three subsequent one-pot nucleophilic substitutions (the SNACK macrocyclisation followed by a displacement of the remaining C6 fluorine with pyrrolidine) delivered the grossly substituted macrocyclic pyrimidine **M43**. A less nucleophilic morpholine **N15** required prolonged heating (65 h) at 150 °C to achieve acceptable conversion of the macrocyclisation step, but despite such harsh conditions the required macrocycle **M44** was isolated in a respectable 51% yield.

For **M28** we observed the formation of two isomeric macrocyclic products at the macrocyclisation step. In this experiment the isomer ratio was improving with reaction time. We hypothesised that this was due to the presence of the chloro substituent at the 5-position of the pyrimidine ring, which in the presence of the *ortho*-substituted aniline motif can create a steric clash between the chlorine and the ether oxygen, thus restricting conformational changes of the macrocyclic ring (Fig. 1). Restricted ring interconversion can lead to formation of a new chiral centre, similar to the formation of chiral atropisomers in rotationally restricted biaryls.[23] In the presence of an another chiral centre (as in the pyrrolidine **M28**) two distinctive diastereoisomers may be observed. Thus we postulated that in SNACK macrocyclisations involving heterocyclic

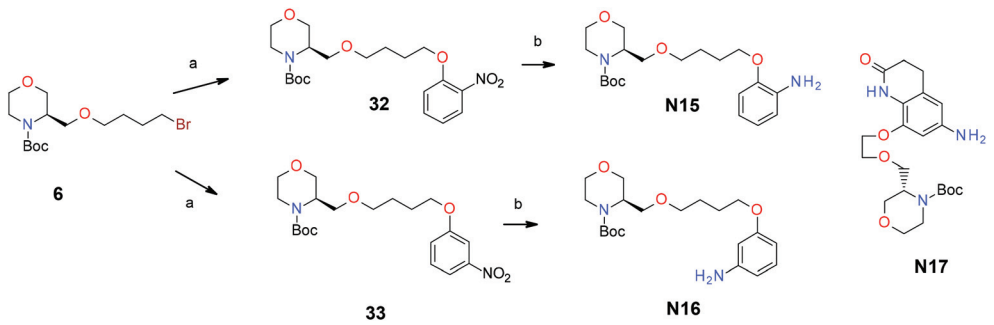

Scheme 11 (a) 3-Nitrophenol or 2-nitrophenol, Cs_2CO_3, DMA, 80 °C, 47% for **32**, 34% for **33**; (b) $HCOONH_4$, Pd/C, EtOH, 80 °C, 100% for **N15**, 100% for **N16**; **N17** prepared as described.[9b]

reagents with a substituent residing between two electrophilic sites formation of a new chiral centre could be plausible.

In the case of reaction between both a symmetrical diamine and a symmetrical dihalo-heterocycle, an achiral macrocycle **34** will form, independently of the size of the R^2 substituent (Scheme 12). In the case, when R^2 relatively is small (*e.g.* H or F), then macrocyclic ring interconversion can easily occur. When R^2 in **34** is larger the ring interconversion may be restricted, but **34** has a plane of symmetry and is superimposable on its mirror image. The situation should change when one or both fragments (diamine and heterocycle) of the macrocycle become unsymmetrical. For example, in the case of combination of a symmetrical diamine unit and an unsymmetrically substituted pyridazine ring. With a relatively small *endo*-cyclic R^2 (**35**) the ring interconversion should still be fairly fast at room temperature. Thus **35** can be considered as an achiral molecule. By increasing the molecular volume of R^2, or alternatively decreasing size of the macrocyclic ring, interconversion in **36** may become more restricted making this molecule chiral. Thus, **36** should exist in two enantiomeric forms **37** and **38**. Similarly, when an unsymmetrical diamine motif is linked to a symmetrically substituted pyrimidine with a relatively small *endo*-cyclic R^2 (**39**) the ring interconversion should be fast at room temperature. Thus, **39** should be considered as achiral. In turn, increasing R^2 size can block ring interconversion in **40**, thus making this macrocycle chiral. Again, it should be possible to separate the racemic **40** into two enantiomers **41** and **42**. Incorporation of another stereo-defined

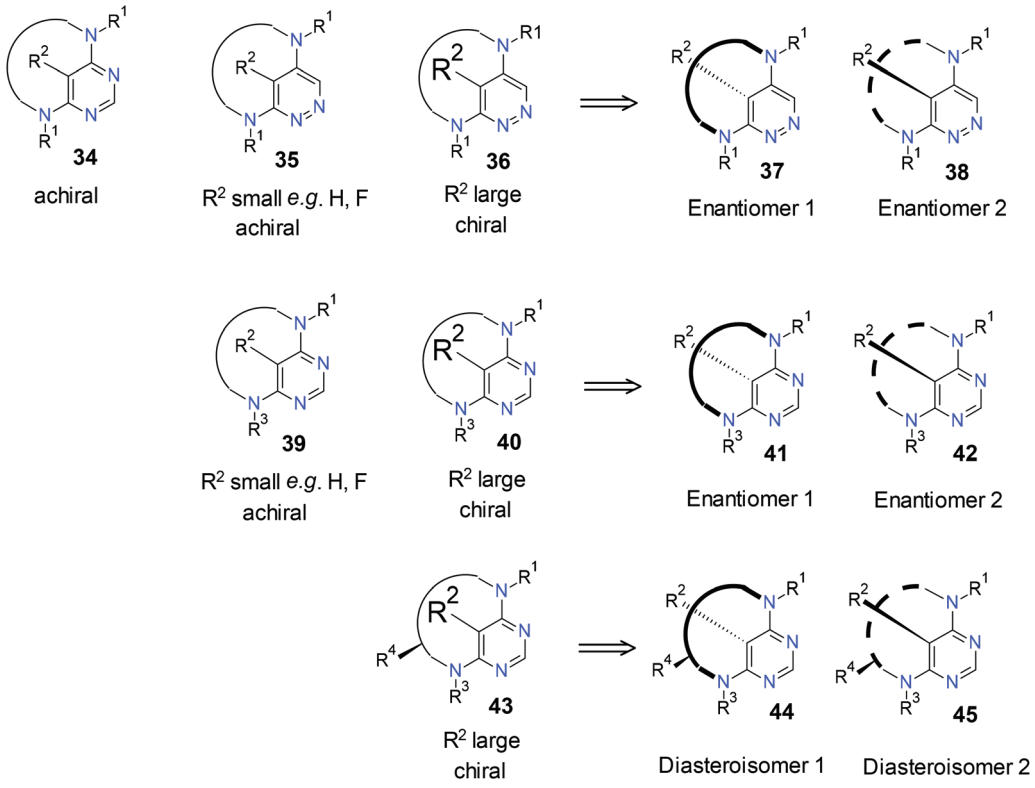

Scheme 12 Formation of a new chiral centre during SNACK macrocyclisations.

chiral centre (R^4 in **43**) into the diamine should allow formation of 2 distinctive diastereoisomeric macrocycles **44** and **45**. We assumed that this was the case with observation of two isomeric products in **M28**. Under the reaction conditions (120 °C) the initial kinetic macrocycle underwent slow equilibration to enrich the mixture with the most stable thermodynamic diastereoisomer. Interestingly, only one isomer was detected for the isomeric macrocycle **M24**. We hypothesised that in **M24** the negative steric interaction between the chlorine atom and the ether oxygen was removed by moving the ether substituent from the *ortho* to *meta* position of the phenyl ring (Fig. 2). With the inner cavity of the macrocyclic ring potentially being large enough to accommodate the chlorine atom the energy barrier would be greatly reduced allowing relatively free interconversion of the macrocyclic ring. This would eliminate the effect of planar chirality and a single isomer can be anticipated. Similarly, only one isomer was observed for some other macrocycles bearing *endo*-cyclic substituents. This was the case for both 16-membered rings in **M23** and **M31** (R_{endo} = F) as well as for the 18-membered macrocycle **H42** (R_{endo} = CN).

To check if stable macrocyclic diastereoisomers can be formed, we investigated the reaction between the amine **N4** and 5-cyano-4,6-dichloro-pyrimidine (**H21**). We were pleased to find that SNACK macrocyclisation between the amine **N4** and 5-cyano-4,6-dichloro-pyrimidine (**H21**) led to formation of a ~2 : 1 mixture of 2 isomers in 37% yield. Both isomers were successfully separated using preparative reverse-phase HPLC to afford two stable diastereoisomeric compounds **M45-1** and **M45-2** (Table 3). No isomer interconversion (epimerisation) was observed at room temperature. To determine the structural identity of each diastereoisomer we used a complementary NMR and computational approach. NOE data was collected for the rotamers using 2D ROESY experiments and the interproton distances were extracted from the intensities of the cross peaks. The conformational landscape of the diastereoisomers was explored independently of the NMR using low mode molecular dynamics methods resulting in a set of conformers for each isomer. The experimentally derived constraint sets for each rotamer (in the form of distances) were combined alternatively with the two sets of conformers using the MSpin software. It was found that the NMR data for Isomer 1 agreed best with structure **M45-1** below, and Isomer 2 with structure **M45-2** (Fig. 3). The NOEs from the CH proton in the pyrrolidine ring were key to differentiate between these isomers. For **M45-2** the pyrrolidine C3–H, a NOE with the aromatic H pointing inwards and with both protons in the double bond is observed, whilst for the same C3–H in the diastereoisomer **M45-1** only the NOE with one of the double bond protons is detected and no NOE is observed with the aromatic CH.

Likewise, ethyl 4,6-dichloropyrimidine-5-carboxylate (**H23**) reacted with **N4** to form a ~2 : 1 mixture of two stable macrocycles **M46-1** and **M46-2**, although in low yield. A similar result was obtained when **N6** was coupled with **H21** to give a mixture of **M47-1** and **M47-2** (ratio ~3 : 1). On the contrary, high chemical yields (>77%) were achieved in reactions between *ortho*-substituted anilines **N5** or **N15** and 5-cyano-4,6-dichloro-pyrimidine (**H21**). Two pairs of 15-membered macrocycles **M48-1**/**M48-2** and **M49-1**/**M49-2** were obtained in equal amount. Similarly, macrocyclisation of **N16** with **H21** was very efficient providing a 3 : 1 mixture of 15-membered diastereoisomeric macrocycles **M50-1** and **M50-2** in high 81% yield. Contrary, SNACK macrocyclisation between **H21** and the ethylene linked di-nucleophile **N17** [9b] was sluggish delivering a 3 : 1 mixture of isomeric **M51-1** and **M51-2** in only 18% yield. The reaction between **N13** and **H21** gave a 1.1 : 1 mixture of 17-membered macrocycles **M52-1** and **M52-2**. Both isomers were successfully separated using achiral SFC. However, gradual erosion of diastereoisomeric purity of collected fractions was observed in solution at room temperature measured by LCMS. Attempts to isolate separated isomers **M52-1** and **M52-2** from SFC fractions lead to equilibration. As shown in Fig. 4 the major isomer **M52-1** easily equilibrated to the 1.1 : 1 mixture of diastereoisomers within 4 days at rt.

Increasing the size of the substituent at the 4-position of the pyrimidine (switching from CN in **H21** to CO_2Et in **H23**)

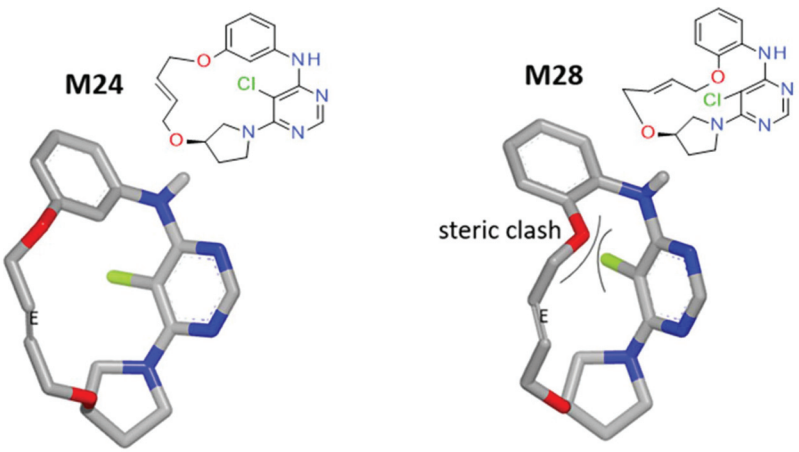

Fig. 2 Restricted interconversion of the macrocyclic ring in **M28**.

Table 3 Formation of atropisomers during SNACK macrocyclisation

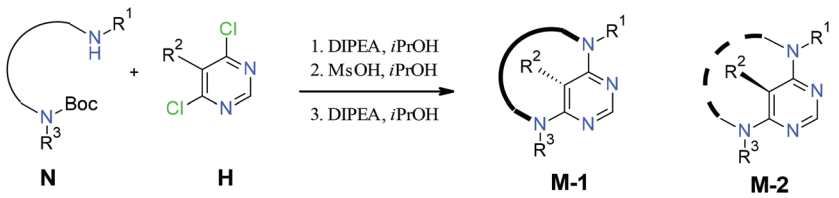

Di-nucleophile	Heterocycle No	R^2	Macrocycle No	Isomer **1**	Isomer **2**	Ring size	Yield (%)	Isomer ratio **1 : 2**
N4	**H21**	CN	**M45-1** **M45-2**	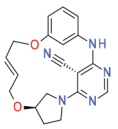	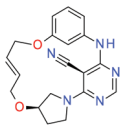	16	37	2 : 1
N4	**H23**	CO_2Et	**M46-1** **M46-2**	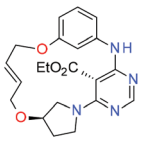	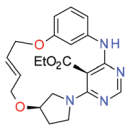	16	14	2 : 1
N6	**H21**	CN	**M47-1** **M47-2**	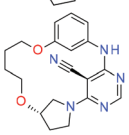	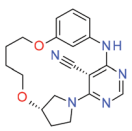	16	26	3 : 1
N5	**H21**	CN	**M48-1** **M48-2**	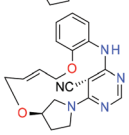	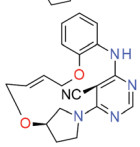	15	80	1 : 1
N15	**H21**	CN	**M49-1** **M49-2**	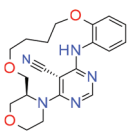	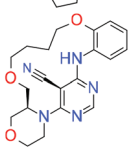	15	77	1 : 1
N16	**H21**	CN	**M50-1** **M50-2**	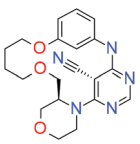	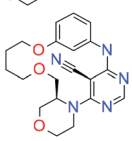	16	81	3 : 1
N17	**H21**	CN	**M51-1** **M51-2**	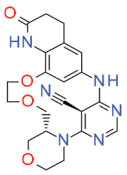	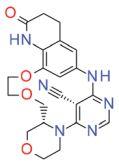	14	18	3 : 1
N13	**H21**	CN	**M52-1** **M52-2**	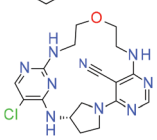	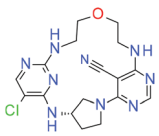	17	36	1 : 1.1
N13	**H23**	CO_2Et	**M53-1** **M53-2**	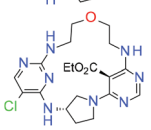	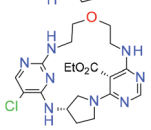	17	46	2 : 3

blocked interconversion of the macrocyclic ring and the pair of stable diastereoisomeric macrocycles **M53-1** and **M53-2** was obtained. Similar atropisomerism due to restricted bond rotation in macrocycles has aslo been observed and reported by others.[24]

Synthesis of BCL6 inhibitors

This SNACK macrocyclisation approach was particularly valuable in the discovery and evaluation of high affinity binders of macrocyclic B-cell lymphoma 6 (BCL6).[9a,b] BCL6 is a transcrip-

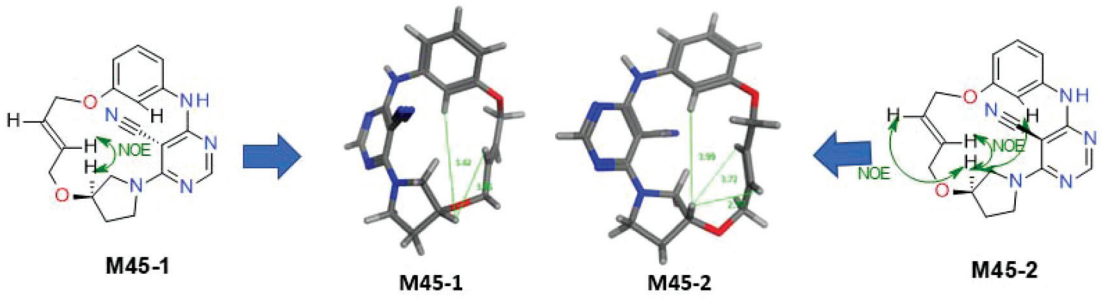

Fig. 3 Conformational analysis (in solution) for diastereoisomers **M45-1** and **M45-2**.

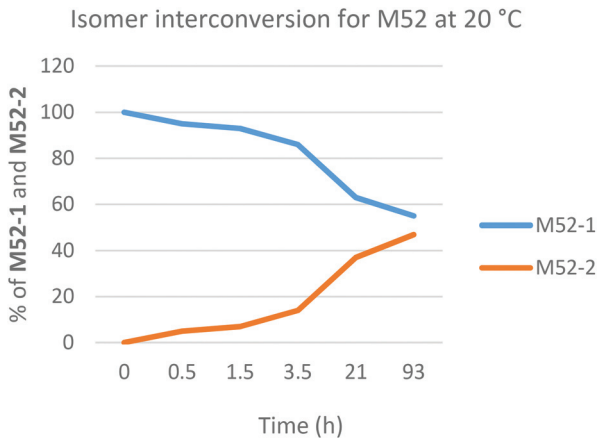

Fig. 4 Equilibration of major isomer **M52-1** to a mixture of diastereomers.

tional repressor required for germinal centre formation and maintenance during the humoral immune response. Inhibition of the protein-protein interaction (PPI) between BCL6 and corepressors has been implicated as a therapeutic target in diffuse large B-cell lymphoma (DLBCL) cancers. Thus potent and selective BCL6 inhibitors were highly attractive targets. To design small molecule high affinity ligands, we used a macrocyclisation strategy to improve binding affinity of our initial "acyclic" leads by increasing the proportion of conformers close to the bioactive conformation. SNACK macrocyclisation greatly facilitated access to diverse macrocyclic frameworks and allowed rapid exploration of structure–activity relationship (SAR) of macrocyclic BCL6 inhibitors. BCL6–ligand complex crystal structures revealed a close proximity between the central heteroaromatic ring of the ligand and the protein backbone, thus indicatating a relatively tight space to accommodate substitution. To evaluate the effect of the substitution of the central heteroaromatic ring on binding to the BTB domain homodimer a set of pyrimidine based macrocycles (**M62–M70**) was prepared starting from the aniline **N18** as drawn in Scheme 13. SNACK macrocyclisation with differently substituted halo-pyrimidines delivered corresponding Cbz-protected macrocyclic piperazines (**M54–M61**) in good yields (38–78%). It's worth noting, that the reaction between **N18** and corresponding heterocycles **H2**, **H10**, **H22**, **H24** or **H27** afforded expected macrocycles (**M54**, **M58**, **M59** or **M61**, respectively), alongside of regioisomeric macrocycles (**M54a**, **M58a**, **M59a** or **M61a**). In the case of **M54**, **M58**, **M59**, formation of the regioisomeric products was attributed to reduced regioselectivity of the first nucleophilic aromatic substitution between the 4- *vs*. 2-position of the pyrimidine ring in **H2**, **H10** or **H22**. Isomeric **M61** and **M61a** formed as a result of the competitive reactivity of both remaining electrophilic centres in the final macrocyclisation step. Removal of Cbz-protection in **M54–M61** with 33% hydrobromic acid in acetic acid followed by reductive amination with formaldehyde yielded the *N*-methylated piperazine derivatives **M62–M69**. Subsequent displacement of the fluorine in **M67** with dimethylamine smoothly afforded the macrocycle **M70** in quantitative yield.

We tested these macrocycles (**M62–M70**) and the known reference BCL6 inhibitior **FX1** [25] in both biochemical and cell-based assays for BCL6 activity (Table 4).[9a] A derivative **M62** that is unsubstituted at the 5- and 6-position of pyrimidine displayed low-micromolar affinity to BCL6 and encouraging activity in the cell reporter assay. 26-Fold improvement in binding affinity was observed for the 5-fluoro-pyridimine **M63** as well as 5-fold increase in cell potency. Further improvement in both BCL6 affinity and cell potency was seen for the 5-chloro-pyridimine **M64** (BCL6 FRET IC_{50} 30 nM). Larger substituents at the 5-position such as bromine (**M65**) and cyano (**M66**) were less tolerated and led to lower BCL6 affinity (3-fold and 8-fold, respectively). Interestingly, despite lower binding affinity, **M66** was equipotent to **M64** in the cell reporter assay. An additional fluorine at the 6-position of pyrimidine in **M67** further increased BCL6 affinity in comparison to 5-chloro-pyridimine **M64** (BCL6 FRET IC_{50} 9 nM) as well as cell potency (BCL6 cell IC_{50} 720 nM). The 5,6-difluoro-pyrimidine **M68** was 10-fold less active in the FRET assay than **M67**. Larger substituents at the 6-position reduced activity. 6-Chloro-5-fluoro-pyrimidine **M69** was only slightly less active than **M68**. However, larger substituents such as 6-dimethylamino in **M70** led to a significant drop in activity. Opportunistically, we also tested selected *N*-Cbz-protected piperazine intermediates **M56**, **M57** and **M60**. Despite showing encouraging binding to BCL6 these compounds were inactive in the cell-based assay. A drop-off from FRET affinity to cell potency is to be expected since the FRET assay is a biochemical assay measuring affinity to BCL6

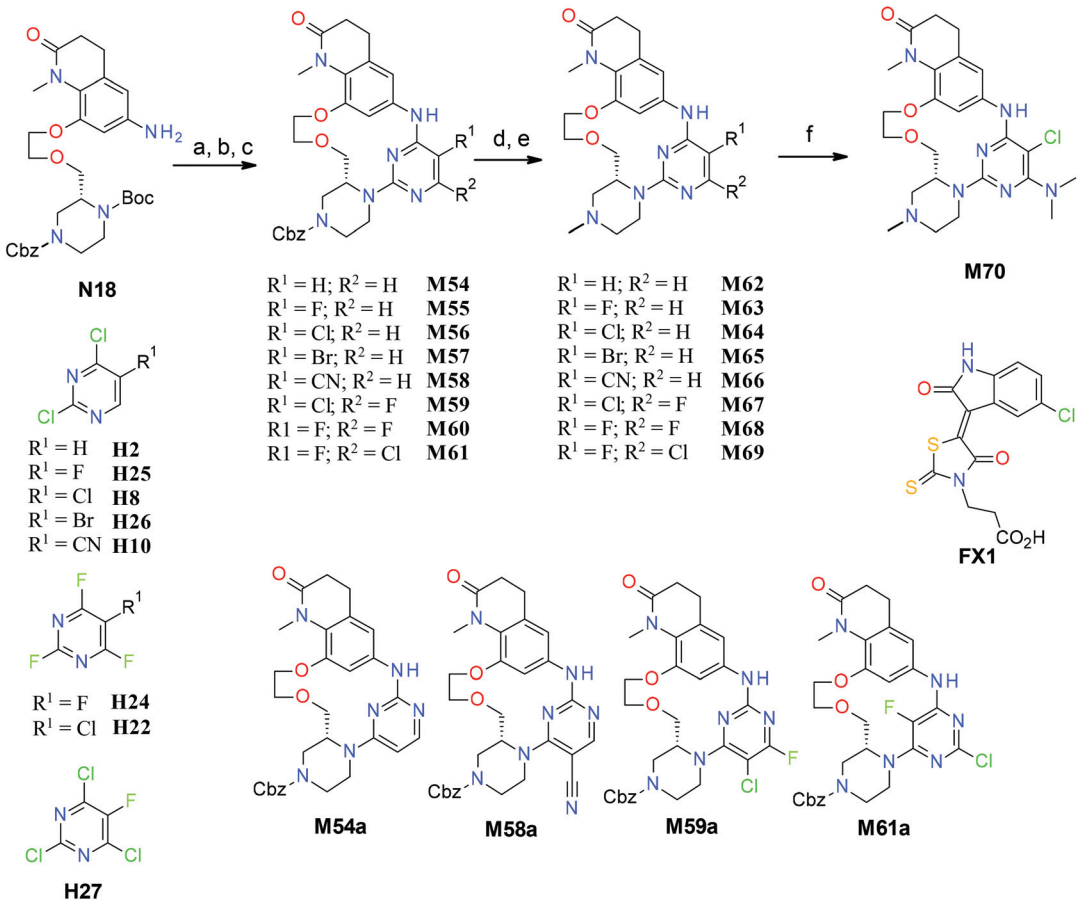

Scheme 13 (a) **N18**,[9b] heterocycle (**H**), iPr_2EtN, iPrOH, 20–80 °C; (b) MsOH, iPrOH, 60–80 °C; (c) iPr_2EtN, iPrOH, 120–150 °C; 57% for **M54** and 3% for **M54a**, 49% for **M55**, 66% for **M56**, 63% for **M57**, 24% for **M58** and 14% for **M58a**, 76% for **M59** and **M59a**, 78% for **M60**, 43% for **M61** and 11% for **M61a** (overall yield for 3 steps) (d) 33% HBr, AcOH, rt; (e) CH_2O_{aq}, $NaCNBH_3$, MeOH; 62% for **M62**, 80% for **M63**, 85% for **M64**, 85% for **M65**, 60% for **M66**, 65% for **M67**, 60% for **M68**, 81% for **M69** (overall yield for 2 steps); (f) Me_2NH, THF, rt, quant.; **N24** prepared as described.[9b]

Table 4 SAR of macrocyclic inhibitors of BCL6

Macrocycle	SNACK yield (%)	BCL6 inhibitor	BCL6 FRET IC_{50} (μM) ± SD[a]	BCL6 cell IC_{50} (μM) ± SD[a]	log $D_{7.4}$
M54; M54a	60[b]	**M62**	3.4 ± 2.7	17 ± 9.6[c]	2.5
M55	49	**M63**	0.13 ± 0.1	2.4 ± 0.4	2.5
M56	66	**M64**	0.029 ± 0.028	1.4 ± 0.08	3.0
M57	63	**M65**	0.23 ± 0.09	2.3 ± 1.0	3.3
M58; M58a	38[b]	**M66**	0.24 ± 0.06	1.4 ± 0.15	2.4
M59; M59a	76[b]	**M67** [9a]	0.009 ± 0.002	0.72 ± 0.17	3.5
M60	78	**M68**	0.096 ± 0.04	2.9 ± 0.9	3.2
M61; M61a	53[b]	**M69**	0.17 ± 0.13	2.1 ± 0.9	3.6
n/a	n/a	**M70**	5.1[d]	15[d]	3.2[e]
n/a	n/a	**FX1** [25]	49	>30	2.2

[a] IC_{50} values are mean values of >3 independent experiments unless otherwise stated, SD = standard deviation; for the assay protocols see ref. 9*a* and *b*. [b] Combined yield for both macrocyclic regioisomers. [c] $n = 2$. [d] $n = 1$. [e] Calculated log $D_{7.4}$.

in competition with a truncated form of the co-repressor peptide SMRT-2 whereas in the cell assay full length versions of any of the BCL6 binding co-repressor peptides will be present and competing for binding to BCL6. All *N*-methyl-piperazines **M62–M70** resided in an acceptable lipophilicity space (log $D_{7.4} < 3.6$).

Conclusions

In summary, a diversity-orientated, efficient macrocyclisation approach based on the double aromatic nucleophilic substitution (SNACK) was developed. This methodology benefited from a large set of diverse commercially available heterocyclic

reagents and allowed a facile incorporation of heterocyclic templates into macrocyclic rings. Using our SNACK macrocyclisation procedure a significant number of structurally diverse macrocycles were prepared to support AstraZeneca internal medicinal chemistry projects. The SNACK reaction enables synthesis of stable diastereoisomers and enantiomers of conformationally restricted macrocycles (atropisomers). The structural identity of the pair of selected diastereoisomers was confirmed by complementary NMR studies and computational methods. SNACK macrocyclisation was particularly valuable in the identification of high affinity binders of B-cell lymphoma 6 with the macrocycle **M67** displaying low-nanomolar affinity to BCL6.

Conflicts of interest

There are no conflicts to declare.

Acknowledgements

The authors would like to thank Eva Lenz, Dan Rhodes, Emma Gates, Paul Davies, David Longmire, Neil Summer and Matthew Sanders for providing analytical support, and Erin Code and Erica Banks for generating biological data.

References

1 A. K. Yudin, (the thematic issue editor), *Chem. Rev.*, 2019, **119**(17), 9723–10392.

2 (*a*) E. Marsault and M. L. Peterson, *J. Med. Chem.*, 2011, **54**, 1961; (*b*) E. Marsault, *Diversity–Oriented Synthesis: Basics and Applications in Organic Synthesis, Drug Discovery and Chemical Biology*, 2013, ch. 8, p. 253; (*c*) A. Whitty, L. A. Viarengo and M. Zhong, *Org. Biomol. Chem.*, 2017, **15**, 7729.

3 (*a*) D. C. Doak, B. Over, F. Giordanetto and J. Kihlberg, *Chem. Biol.*, 2014, **21**, 1115; (*b*) F. Giordanetto and J. Kihlberg, *J. Med. Chem.*, 2014, **57**, 278.

4 (*a*) S. Vendeville and M. D. Cummings, *Annu. Rep. Med. Chem.*, 2013, **48**, 371; (*b*) M. D. Cummings and S. Sekharan, *J. Med. Chem.*, 2019, **62**, 6843; (*c*) E. M. Driggers, S. P. Hale, J. Lee and N. K. Terrett, *Nat. Rev. Drug Discovery*, 2008, **7**, 608; (*d*) P. Ermert, *Chimia*, 2017, **71**, 678.

5 (*a*) T. A. F. Cardote and A. Ciulli, *ChemMedChem*, 2016, **11**, 787; (*b*) A. D. G. Lawson, M. MacCoss and J. P. Heer, *J. Med. Chem.*, 2018, **61**, 4283; (*c*) P. G. Dougherty, Z. Qian and D. Pei, *Biochem. J.*, 2017, **474**, 1109; (*d*) B. C. Doak, J. Zheng, D. Dobritzsch and J. Kihlberg, *J. Med. Chem.*, 2016, **59**, 2312.

6 (*a*) E. Valeur, S. M. Guéret, H. Adihou, R. Gopalakrishnan, M. Lemurell, H. Waldmann, T. N. Grossmann and A. T. Plowright, *Angew. Chem., Int. Ed.*, 2017, **56**, 10294; (*b*) I. Collins and J. Mallinson, *Future Med. Chem.*, 2012, **4**, 1409.

7 A. K. Yudin, *Chem. Sci.*, 2015, **6**, 30.

8 (*a*) J. W. Johannes, S. Bates, C. Beigie, M. A. Belmonte, J. Breen, S. Cao, P. A. Centrella, M. A. Clark, W. J. Cuozzo, C. E. Dumelin, A. D. Ferguson, S. Habeshian, D. Hargreaves, C. Joubran, S. Kazmirski, A. D. Keefe, M. L. Lamb, H. Lan, Y. Li, H. Ma, S. Mlynarski, M. J. Packer, P. B. Rawlins, D. W. Robbins, H. Shen, E. A. Sigel, H. H. Soutter, N. Su, D. M. Troast, H. Wang, K. F. Wickson, C. Wu, Y. Zhang, Q. Zhao, X. Zheng and A. W. Hird, *ACS Med. Chem. Lett.*, 2017, **8**, 239; (*b*) A. Y. S. Balazs, R. J. Carbajo, N. L. Davies, Y. Dong, A. W. Hird, J. W. Johannes, M. L. Lamb, W. McCoull, P. Raubo, G. R. Robb, M. J. Packer and E. Chiarparin, *J. Med. Chem.*, 2019, **62**, 9418.

9 (*a*) W. McCoull, R. D. Abrams, E. Anderson, K. Blades, P. Barton, M. Box, J. Burgess, K. Byth, Q. Cao, C. Chuaqui, R. J. Carbajo, T. Cheung, E. Code, A. D. Ferguson, S. Fillery, N. O. Fuller, E. Gangl, N. Gao, M. Grist, D. Hargreaves, M. R. Howard, J. Hu, P. D. Kemmitt, J. E. Nelson, N. O'Connell, D. B. Prince, P. Raubo, P. B. Rawlins, G. R. Robb, J. Shi, M. J. Waring, D. Whittaker, M. Wylot and X. Zhu, *J. Med. Chem.*, 2017, **60**, 4386; (*b*) W. McCoull, T. Cheung, E. Anderson, P. Barton, J. Burgess, K. Byth, Q. Cao, M. P. Castaldi, H. Chen, E. Chiarparin, R. J. Carbajo, E. Code, S. Cowan, P. R. Davey, A. D. Ferguson, S. Fillery, N. O. Fuller, N. Gao, D. Hargreaves, M. R. Howard, J. Hu, A. Kawatkar, P. D. Kemmitt, E. Leo, M. D. Molina, N. O'Connell, P. Petteruti, T. Rasmusson, P. Raubo, P. B. Rawlins, P. Ricchiuto, G. R. Robb, M. Schenone, M. J. Waring, M. Zinda, S. Fawell and D. M. Wilson, *ACS Chem. Biol.*, 2018, **13**, 3131.

10 J. G. Kettle, H. Alwan, M. Bista, J. Breed, N. L. Davies, K. Eckersley, S. Fillery, K. M. Foote, L. Goodwin, D. R. Jones, H. Käck, A. Lau, J. W. M. Nissink, J. Read, J. S. Scott, B. Taylor, G. Walker, L. Wissler and M. Wylot, *J. Med. Chem.*, 2016, **59**, 2346.

11 V. Martí-Centelles, M. D. Pandey, M. I. Burguete and S. V. Luis, *Chem. Rev.*, 2015, **115**, 8736.

12 (*a*) H. Itoh and M. Inoue, *Org. Biomol. Chem.*, 2019, **17**, 6519; (*b*) J. H. Lee, H.-S. Kim and H.-S. Lim, *Org. Lett.*, 2011, **13**, 5012.

13 S. Collins, S. Bartlett, F. Nie, H. F. Sore and D. R. Spring, *Synthesis*, 2016, **48**, 1457.

14 (*a*) C. M. Madsen and M. H. Clausen, *Eur. J. Org. Chem.*, 2011, 3107; (*b*) I. V. Smolyar, A. K. Yudin and V. G. Nenajdenko, *Chem. Rev.*, 2019, **119**, 10032; (*c*) X. Yu and D. Sun, *Molecules*, 2013, **18**, 6230; (*d*) A. M. Webster and S. L. Cobb, *Chem. – Eur. J.*, 2018, **24**, 7560.

15 (*a*) K. T. Mortensen, T. J. Osberger, T. A. King, H. F. Sore and D. R. Spring, *Chem. Rev.*, 2019, **119**, 10288; (*b*) S. J. Kaldas and A. K. Yudin, *Chem. – Eur. J.*, 2018, **24**, 7074; (*c*) C. J. White and A. K. Yudin, *Nat. Chem.*, 2011, **3**, 509.

16 (*a*) L. A. Wessjohann, D. G. Rivera and O. E. Vercillo, *Chem. Rev.*, 2009, **109**, 796; (*b*) L. Reguera and D. G. Rivera, *Chem. Rev.*, 2019, **119**, 9836; (*c*) R. Hili, V. Rai and A. K. Yudin,

J. Am. Chem. Soc., 2010, **132**, 2889; (*d*) E. M. M. Abdelraheem, S. Shaabani and A. Dömling, *Synlett*, 2018, **29**, 1136; (*e*) E. M. M. Abdelraheem, M. P. de Haan, P. Patil, K. Kurpiewska, J. Kalinowska-Tłuścik, S. Shaabani and A. Dömling, *Org. Lett.*, 2017, **19**, 5078; (*f*) E. M. M. Abdelraheem, K. Kurpiewska, J. Kalinowska-Tłuścik and A. Dömling, *J. Org. Chem.*, 2016, **81**, 8789; (*g*) M. Paira, *Chem. Biol. Interface*, 2019, **9**, 186; (*h*) E. M. M. Abdelraheem, S. Khaksar and A. Dömling, *Synthesis*, 2018, **50**, 1027.

17 (*a*) B. K. Vriesema, J. Buter and R. M. Kellogg, *J. Org. Chem.*, 1984, **49**, 110; (*b*) V. Martí-Centelles, M. I. Burguete and S. V. Luis, *Chem. – Eur. J.*, 2012, **18**, 2409.

18 (*a*) G. Sandford, *Chem. – Eur. J.*, 2003, **9**, 1464; (*b*) U. Lücking, G. Siemeister, M. Schäfer, H. Briem, M. Krüger, P. Lienau and R. Jautelat, *ChemMedChem*, 2007, **2**, 63; (*c*) D. Scharn, L. Germeroth, J. Schneider-Mergener and H. Wenschuh, *J. Org. Chem.*, 2001, **66**, 507; (*d*) J. K. Loh, N. Asad, T. B. Samarakoon and P. R. Hanson, *J. Org. Chem.*, 2015, **80**, 9926.

19 (*a*) R. D. Taylor, M. MacCoss and A. G. D. Lawson, *J. Med. Chem.*, 2014, **57**, 5845; (*b*) E. Vitaku, D. T. Smith and J. T. Njardarson, *J. Med. Chem.*, 2014, **57**, 10257.

20 (*a*) H. S. Soor, S. D. Appavoo and A. K. Yudin, *Bioorg. Med. Chem.*, 2018, **26**, 2774; (*b*) J. R. Frost, C. C. G. Scully and A. K. Yudin, *Nat. Chem.*, 2016, **8**, 1105.

21 D. G. Brown and J. Boström, *J. Med. Chem.*, 2016, **59**, 4443.

22 J. C. Collins and K. James, *MedChemComm*, 2012, **3**, 1489.

23 G. Bringmann, A. J. Price Mortimer, P. A. Keller, M. J. Gresser, J. Garner and M. Breuning, *Angew. Chem., Int. Ed.*, 2005, **44**, 5384.

24 (*a*) E. Van Den Berge, J. Pospíšil, T. Trieu-Van, L. Collard and R. Robiette, *Eur. J. Org. Chem.*, 2011, 6649; (*b*) P. W. Glunz, L. Mueller, D. L. Cheney, V. Ladziata, Y. Zou, N. W. Wurtz, A. Wei, P. C. Wong, R. R. Wexler and E. S. Priestley, *J. Med. Chem.*, 2016, **59**, 4007; (*c*) J. Elleraas, J. Ewanicki, T. W. Johnson, N. W. Sach, M. R. Collins and P. F. Richardson, *Angew. Chem., Int. Ed.*, 2016, **55**, 3590; (*d*) C. Roussel, N. Vanthuyne, N. Shineva, M. Bouchekara and A. Djafric, *ARKIVOC*, 2008, (VIII), 28.

25 Literature BCL6 inhibitor (**FX1**): A. Melnick, L. C. A. Cerchietti, M. G. Cardenas, F. Xue and A. D. Mackerell, WO 2014204859, 2014; Y. Ai, L. Hwang, A. D. MacKerell, A. Melnick and F. Xue, *J. Med. Chem.*, 2021, **64**, 4333.